Letter

Vol. 46, No. 13 / 1 July 2021 / *Optics Letters* 3115

Optics Letters

Double-pass pre-chirp managed amplification with high gain and high average power

Yao Zhang,[1,2] Jingshang Wang,[2,3] Hao Teng,[2,3,4] Shaobo Fang,[2,3,4] Junli Wang,[1,5] Guoqing Chang,[2,3,4,6] and Zhiyi Wei[2,3,4,7]

[1]School of Physics and Optoelectronic Engineering, Xidian University, Xi'an 710071, China
[2]Beijing National Laboratory for Condensed Matter Physics, Institute of Physics, Chinese Academy of Sciences, Beijing 100190, China
[3]University of Chinese Academy of Sciences, Beijing 100049, China
[4]Songshan Lake Materials Laboratory, Dongguan, Guangdong 523808, China
[5]e-mail: dispersion@126.com
[6]e-mail: guoqing.chang@iphy.ac.cn
[7]e-mail: zywei@iphy.ac.cn

Received 16 April 2021; revised 26 May 2021; accepted 2 June 2021; posted 2 June 2021 (Doc. ID 428066); published 23 June 2021

We demonstrate, to the best of our knowledge, the first double-pass pre-chirp managed fiber amplifier. The double-pass fiber amplifier exhibits high gain allowing us to amplify chirped picosecond pulses from 20 mW to 113 W in a rod-type Yb-fiber corresponding to 38 dB gain. We study the dependence of static mode degradation (SMD) on the nonlinear phase shift (NPS) accumulated by the amplified pulse. Our results indicate that a larger nonlinear phase shift results in stronger nonlinear polarization evolution of the fundamental mode and leads to a lower threshold for SMD. After optimization, our pre-chirp managed amplifier seeded by 80 mW pulses delivers 102 W amplified power from the main output. The amplified pulses are compressed to 37 (55) fs with 90 (100) W average power by a grating pair (chirped mirrors). The double-pass configuration significantly simplifies the implementation of pre-chirp managed fiber amplifiers leading to an extremely compact system.

https://doi.org/10.1364/OL.428066

The rapid advance of ultrafast Yb-fiber amplifiers largely relies on the development of double-clad large-mode-area Yb-fibers, such as rod-type fibers [1], chirally coupled core fibers [2], leakage channel fibers [3], and tapered fibers [4]. Rod-type Yb-fibers are of particular interest because they can ensure robust single-mode operation, even as their mode-field diameter exceeds 100 µm [5,6]. This attractive feature has made rod-type Yb-fibers a popular candidate for constructing high-power and high-energy ultrafast fiber amplifiers. Most of these amplifiers were configured at a single pass of rod-type Yb-fibers, and few of them employed a double-pass configuration. Compared with a single-pass configuration, double-pass rod-type Yb-fiber amplifiers exhibit much higher gain (>40 dB), and therefore can amplify weak seeding pulses [7–9]. Such a unique feature, together with the large mode area offered by rod-type Yb-fibers allows us to construct powerful femtosecond sources in a compact format. Most recent works have revealed that high-power rod-type Yb-fiber amplifiers at a double pass exhibit two types of instability: static mode degradation (SMD) and dynamic transverse mode instability (TMI) [7–9]. Unlike the dynamic TMI that also exists in single-pass fiber amplifiers, SMD only appears in a double-pass configuration in which the counter-propagating modes establish a thermo-optic index grating causing scattering between co-propagating modes [7]. References [8,9] carefully investigated the effect of seeding power on the SMD and TMI, and found that less seeding power corresponds to a higher SMD threshold and therefore allows the generation of higher average power. More specifically, 10 mW 20 ps seeding pulses were amplified to 113-W with >40 dB gain prior to the onset of SMD [9].

To date, all the demonstrated double-pass fiber amplifiers are either seeded by narrowband picosecond pulses to study the power scalability or seeded by strongly stretched broadband pulses to achieve chirped-pulse amplification (CPA) [8–12]. In this Letter, we demonstrate for the first time, to the best of our knowledge, pre-chirp managed amplification (PCMA) in a double-pass rod-type Yb-fiber amplifier. PCMA is a nonlinear amplification technique that can amplify femtosecond pulses with the spectral width exceeding the gain bandwidth of a fiber amplifier [13–17]. In a PCMA system, the pulse prior to amplification is properly pre-chirped to the duration of a sub-picosecond. In the subsequent fiber amplifier, the pre-chirped seeding pulse acquires a large amount of a nonlinear phase shift (NPS), and the optical spectrum is substantially broadened with a bandwidth that can support transform-limited pulses with the duration well below 100 fs [13]. When implemented in rod-type Yb-fiber amplifiers, PCMA allows the generation of microjoule-level, tens of femtosecond pulses with ∼100 W average power. However, due to a relatively low gain (∼20 dB) in a single-pass rod-type Yb-fiber amplifier, single-pass PCMA requires Watt-level seeding pulses with tens of nanojoule pulse energy. To date, these seeding pulses for all the demonstrated high-power (>50 W) Yb-fiber PCMA system were obtained from a complicated Yb-fiber CPA system. The work in this Letter serves two purposes: (1) to study the effect of seeding

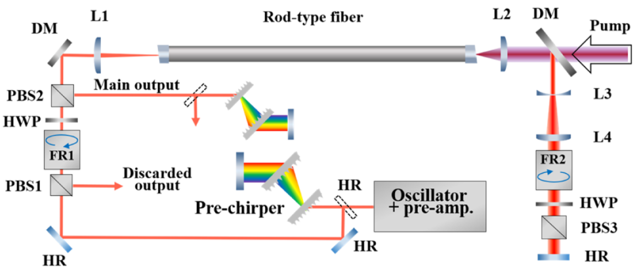

Fig. 1. DP-PCMA system with the pre-chirper located before the forward amplification. HR, high-reflection mirror; PBS, polarization beam splitter; HWP, half-wave plate; DM, dichroic mirror; FR, Faraday rotator; L, lens.

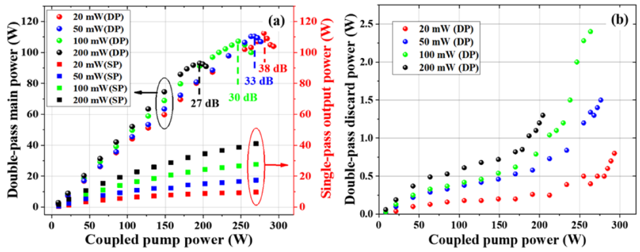

Fig. 2. (a) Double-pass (DP) main-output power and single-pass (SP) output power versus coupled pump power for various seed power. (b) Double-pass discarded power versus coupled pump power for different seed powers.

pulse duration on SMD and (2) to demonstrate that double-pass PCMA (DP-PCMA) provides much simplified design and more flexibility compared with single-pass PCMA.

Figure 1 shows the schematic of our DP-PCMA system. The seed source consists of a mode-locked fiber oscillator and a pre-amplifier, and delivers 44 MHz positively chirped 7 ps pulses centered at 1034 nm. A pair of transmission gratings (1000 l/mm) placed before the power amplifier adds group-delay dispersion (GDD) to pre-chirp the seeding pulses such that the pulse duration can be continuously tuned between 0.2 and 6.5 ps. The power amplifier is constructed from 0.8 m rod-type photonic crystal fiber (NKT, areoGAIN-ROD-PM85). After the rod-type fiber, a dichroic mirror separates the signal from the pump, and a telescope (L3 and L4) expands the beam to avoid the thermal effect. The forward-propagating amplified pulses are then sent back to the amplifier through a Faraday rotator (FR2), a half-wave plate (HWP), a polarization beam splitter (PBS3), and a high-reflection mirror. After a second pass of the rod-type fiber, the backward-propagating amplified pulses are separated into two exit ports: main output and discard output. The pulses at the main output are finally compressed by a pair of transmission gratings.

We adjust the grating-pair-based pre-chirper to compress the pulses at the output of the pre-amplifier to the shortest pulse duration of 0.2 ps. Then we can add different amounts of pre-chirping GDD, either negative or positive, to vary the pulse duration. We add $+0.86\ \mathrm{ps}^2$ GDD to the seeding pulses to stretch them to 6.5 ps in duration, and then we investigate the effect of seeding power on the SMD. The circles in Fig. 2 illustrate the main-output power [Fig. 2(a)] and the discard-output power [Fig. 2(b)] versus coupled pump power at seeding powers of 20 (red), 50 (blue), 100 (green), and 200 mW (black). For all input signal power at a dual-pass configuration, the main-output power increases with the coupled pump power up to a maximum. Once the pump power exceeds a threshold, the main-output power rapidly drops, and meanwhile the discarded power increases exponentially. These results are consistent with those reported in Ref. [8,9] and exhibit the same tendency: seeding a double-pass amplifier with less input power results in a higher SMD threshold and thus allows higher amplified power at the main output. More specific, 20 mW seeding pulses can be amplified up to 113 W corresponding to 38 dB gain when the coupled pump power reaches 276 W. In our DP-PCMA system, dynamic TMI starts to appear as the coupled pump power exceeds 276 W, which is close to the reported threshold of 265 W in Ref. [9].

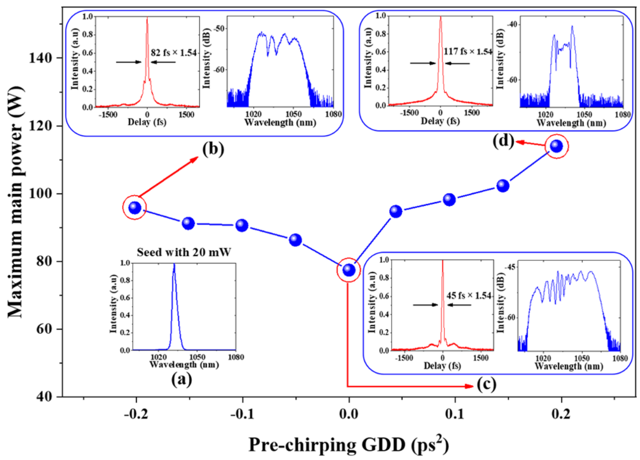

Fig. 3. Maximum main power as a function of pre-chirping GDD with the seeding power at 20 mW. The inset in (a) shows the input seeding spectrum. The output spectra and the autocorrelation traces of the compressed pulses corresponding to pre-chirping GDD at -0.2, 0, and $+0.2\ \mathrm{ps}^2$ are shown in the insets in (b), (c), and (d), respectively.

For comparison, we also show in Fig. 2(a) the single-pass output power versus the coupled pump power for different seeding powers. As expected, a single-pass configuration has much smaller gain and produces less amplified power. In this scenario, the 20 mW seeding pulses are amplified to about 10 W, one order of magnitude less than achieved in the double-pass amplification.

We then fix the seeding power at 20 mw and study the effect of seeding pulse duration on the SMD. We gradually reduce the pre-chirping GDD from $+0.86$ to $+0.2\ \mathrm{ps}^2$. Accordingly, the pulse duration is reduced from 6.5 to 2.3 ps. Despite such a substantial pulse duration reduction, the maximum main-output power is limited by the dynamic TMI and stays at ~113 W at the coupled pump power of 276 W. However, further reducing the pre-chirping GDD to decrease the pulse duration causes a continuously drop of the main-output power. As Fig. 3 shows, the maximum main-output power drops from 113 to 77 W as we reduce the pre-chirping GDD from $+0.2$ to $0\ \mathrm{ps}^2$ corresponding to seeding pulse duration varying from 2.3 to 0.2 ps. As we continue to reduce the pre-chirping GDD from 0 to $-0.2\ \mathrm{ps}^2$, the seeding pulse duration increases from 0.2 to 2.3 ps, and the maximum main-output power increases from 77 to 97 W.

During PCMA, pre-chirping the seeding pulse by adding different amounts of GDD results in different NPSs in the rod-type Yb-fiber which, in turn, leads to broadened spectra with different bandwidths. This is evidenced by the optical spectra at the main output [blue curves in the insets in (b), (c), and (d) of Fig. 3] for the pre-chirping GDD at -0.2, 0, and $+0.2\ \mathrm{ps}^2$. As a comparison, the seeding pulse spectrum is shown in the inset in (a). The red curves in the insets in (b), (c), and (d) plot the autocorrelation traces of the compressed pulses after the grating compressor. Assuming a hyperbolic secant pulse profile, the pulse durations are estimated to be 82, 45, and 117 fs, respectively. As expected, the shortest seeding pulse for pre-chirping GDD at $0\ \mathrm{ps}^2$ accumulates the largest NPS, develops the broadest spectrum, and leads to the shortest compressed-pulse duration. While adding pre-chirping GDD of $+0.2$ or $-0.2\ \mathrm{ps}^2$ gives rise to the same seeding pulse duration, the negatively pre-chirped seeding pulse experiences pulse compression at the beginning of the Yb-fiber amplifier, and thus acquires a larger NPS. Consequently, the amplified spectrum associated with the $-0.2\ \mathrm{ps}^2$ pre-chirping GDD exhibits a broader bandwidth compared with the spectrum corresponding to $+0.2\ \mathrm{ps}^2$ pre-chirping GDD, and thus generates shorter compressed pulses (82 versus 117 fs).

The results in Fig. 3 clearly suggest that a larger NPS leads to less than maximum main-output power, which we believe is caused by nonlinear polarization rotation of the fundamental mode. As the results in Ref. [9] pointed out, due to the coupling between the LP_{01} and LP_{11} modes and the polarization rotation of the LP_{11} mode in the rod-type fiber, the initial linearly polarized LP_{01} mode becomes elliptically polarized. A larger NPS during the PCMA causes stronger nonlinear polarization rotation, which transfers more power to the discarded output. Consequently, the maximum main output drops with an increased NPS.

Besides providing high gain to allow amplifying much weaker seeding pulses, another advantage offered by DP-PCMA over a single-pass configuration is that the pre-chirper in a double-pass configuration can be placed at two possible locations: (1) before the rod-type Yb-fiber prior to the forward amplification (as we have shown in Fig. 1) and (2) behind the fiber prior to the backward amplification. Figure 4 shows the DP-PCMA system in which we place the pre-chirper at the second location. To mitigate an excessive NPS, we add a quarter-wave plate (QWP1) before the rod-type fiber to generate circularly polarized seeding pulses. Our recent results showed that using circularly polarized seeding pulses can reduce the NPS by a factor of 1.5 [18]. After the amplifier, another QWP converts the circularly polarized pulses back to linearly polarized pulses, which are then pre-chirped by the grating pair prior to backward amplification. The amplified pulses at the main output are finally compressed by either a pair of transmission gratings or several high-dispersion mirrors.

During the experiments, we found that the seeding pulse power affects the maximum main-output power as well as the compressed-pulse quality. We experimentally determine that optimal results with both high average power ($\sim$100 W) and excellent pulse quality are obtained, as we set the average power of the seeding pulses at 80 mW. These positively chirped pulses with a duration of $\sim$7 ps are then amplified by the rod-type fiber in forward propagation. As the coupled pump power exceeds 200 W, the forward amplified seeding pulses are spectrally broadened such that they can be compressed by the pre-chirper to the shortest pulse duration less than 150 fs. Then we add

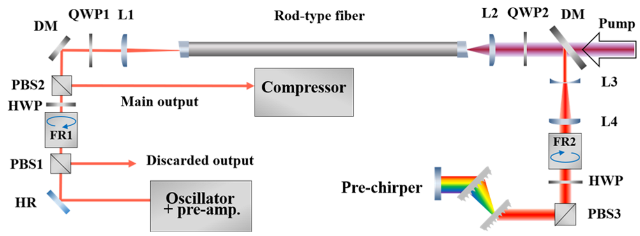

Fig. 4. DP-PCMA system with the pre-chirper located prior to backward amplification. HR, high-reflection mirror; PBS, polarization beam splitter; HWP, half-wave plate; QWP, quarter-wave plate; DM, dichroic mirror; FR, Faraday rotator; and L, lens.

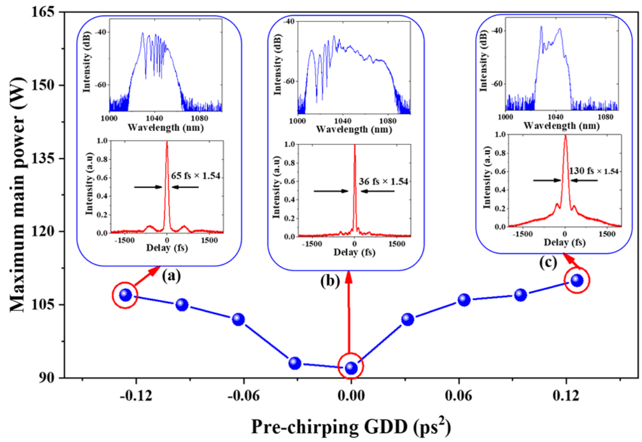

Fig. 5. Maximum main power as a function of pre-chirping GDD with the seeding power at 80 mW. The output spectra and the autocorrelation traces of the compressed pulses corresponding to pre-chirping GDD at -0.125, 0, and $+0.125\ \mathrm{ps}^2$ are shown in the insets in (a), (b), and (c), respectively.

different amounts of pre-chirping GDD to vary the pulse duration prior to the backward amplification. Figure 5 shows the maximum main-output power as the pre-chirping GDD varies from -0.125 to $+0.125\ \mathrm{ps}^2$. Accordingly, the pulse duration prior to the backward amplification varies from 140 fs to 2.1 ps. The results in Fig. 5 are similar to those in Fig. 3; that is, a larger NPS leads to a broader spectrum [blue curves in the insets of (a), (b), and (c) of Fig. 5] with less than maximum main-output power.

The red curves in the insets of (a), (b), and (c) of Fig. 5 plot the autocorrelation traces of the pulses compressed by a pair of transmission gratings. The shortest compressed pulses of 36 fs are achieved for the pre-chirping GDD set at $0\ \mathrm{ps}^2$. However, the average power before the compression is 92 W and becomes 81 W after the grating compressor. Careful experiments show that a higher average power with good compression quality can be achieved by introducing negative pre-chirping GDD. We add $-0.063\ \mathrm{ps}^2$ GDD to the pulses prior to the backward amplification, and the maximum main-output power is 102 W. In this scenario, the 80 mW seeding pulses are amplified to 8.4 W during the forward amplification. Figure 6(a) shows the spectrum prior to the backward amplification (red curve) and the one after the backward amplification (blue curve). The amplified pulses are compressed by a grating pair to 37 fs in duration; the measured autocorrelation trace is shown as the red curve in Fig. 6(b). The black dashed curve in the figure is

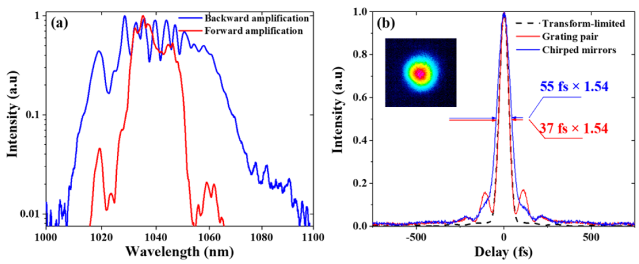

Fig. 6. (a) Forward amplified spectrum (red) and backward amplified spectrum (blue). (b) Autocorrelation trace of the amplified pulse compressed by the grating pair (red) and by chirped mirrors (blue). Black dash curve: autocorrelation trace of a transform-limited pulse. The inset shows the beam profile.

the calculated autocorrelation trace of the transform-limited pulse given by the optical spectrum [i.e., blue curve in Fig. 6(a)]. The grating-pair compressor introduces 12% transmission loss and average power of compressed pulses is 90 W. In our previous work, we show that high-dispersion chirped mirrors with negligible loss can be used as the compressor in a PCMA system [18]. Here we use six pieces of these mirrors to replace the grating pair as the compressor, and the compression efficiency is up to 98%. Therefore, the compressed pulses have an average power of 100 W. However, unlike the grating-pair compressor, using chirped mirrors cannot adjust the GDD continuously; therefore, the compressor pulse duration deviates a bit more from the transform-limited pulse. As the blue curve in Fig. 6(b) shows, the compressed pulse is 55 fs in duration, 18 fs longer than achieved from the grating compressor. The inset of Fig. 6(b) shows the excellent beam profile.

To conclude, we demonstrate the first DP-PCMA, to the best of our knowledge. The double-pass configuration permits us to place the pre-chirper before either the forward amplification or the backward amplification. Thanks to the high gain associated with the double-pass configuration, our rod-type Yb-fiber amplifier can amplify chirped picosecond pulses from 20 mW to 113 W (corresponding to 38 dB gain) limited by dynamic TMI. By pre-chirping the seeding pulses to vary their duration, we investigate the effect of a NPS on SMD. We find that a larger NPS leads to a lower SMD threshold. Although the amplified power is lower compared with single-pass PCMA, the DP-PCMA allows amplifying much weaker seeding pulses. By placing the pre-chirper prior to the backward amplification, we amplify 80 mW seeding pulses and obtain 102 W amplified power from the main output. The amplified pulses are compressed to 37 fs with 90 W average power. When high-dispersion mirrors are used to compress the amplified pulses, we generate 100 W, 55 fs pulses.

DP-PCMA has two advantages. First, the capability to amplify seeding pulses with tens of milliwatt average power substantially simplifies the laser system. Such seeding pulses can be directly generated by a passively mode-locked oscillator. In other words, a DP-PCMA system including an oscillator and a rod-type Yb-fiber can produce 100 W, $\sim$40 fs pulses. Secondly, a double-pass configuration is compatible with divided-pulse amplification (DPA) such that the pulse divider also serves as the pulse recombiner [11,19], and the pulse division/recombination is passively stabilized. In contrast, a single-pass configuration requires a separate recombiner, and normally active stabilization is necessary. Recently, we proposed pre-chirp managed DPA using composite birefringent plates to construct the pulse divider/recombiner. Our simulation showed that such a combination of PCMA and DPA allows the generation of <50 fs pulses with >100 μJ pulse energy and >2 GW peak power [20]. Ongoing work introduces proper composite birefringent plates into our DP-PCMA system and experimentally proves our theoretical work in Ref. [20].

Funding. Key-Area Research and Development Program of Guangdong Province (2018B090904003); National Natural Science Foundation of China (11774234, 12034020, 91950113); Chinese Academy of Sciences (YJKYYQ20190034); National Key Research and Development Program of China (2018YFB1107200, 2020YFB1313702); Open Research Fund of State Key Laboratory of Pulsed Laser Technology; Youth Innovation Promotion CAS (2018007).

Disclosures. YZ, JW, HT, SF, JW, GC, ZW: Institute of Physics, Chinese Academy of Sciences (P) .

Data Availability. Data underlying the results presented in this paper are not publicly available at this time but may be obtained from the authors upon reasonable request.

REFERENCES

1. J. Limpert, N. Deguil-Robin, I. Manek-Hönninger, F. Salin, F. Röser, A. Liem, T. Schreiber, S. Nolte, H. Zellmer, A. Tünnermann, J. Broeng, A. Petersson, and C. Jakobsen, Opt. Express **13**, 1055 (2005).
2. C.-H. Liu, G. Chang, N. Litchinitser, D. Guertin, N. Jacobsen, K. Tankala, and A. Galvanauskas, in *Conference on Lasers and Electro-Optics (CLEO)* (2007).
3. L. Dong, T. Wu, H. A. McKay, L. Fu, J. Li, and H. G. Winful, IEEE J. Sel. Top. Quantum Electron. **15**, 47 (2009).
4. A. Fedotov, T. Noronen, R. Gumenyuk, V. Ustimchik, Y. Chamorovskii, K. Golant, M. Odnoblyudov, J. Rissanen, T. Niemi, and V. Filippov, Opt. Express **26**, 6581 (2018).
5. F. Stutzki, F. Jansen, T. Eidam, A. Steinmetz, C. Jauregui, J. Limpert, and A. Tünnermann, Opt. Lett. **36**, 689 (2011).
6. J. Limpert, F. Stutzki, F. Jansen, H.-J. Otto, T. Eidam, C. Jauregui, and A. Tünnermann, Light Sci. Appl. **1**, e8 (2012).
7. J. Lægsgaard, Opt. Express **24**, 13429 (2016).
8. J. F. Lupi, M. M. Johansen, M. Michieletto, and J. Laegsgaard, Opt. Lett. **43**, 5535 (2018).
9. J.-F. Lupi, M. M. Johansen, M. Michieletto, S. Lønborg Christensen, and J. Lægsgaard, J. Opt. Soc. Am. B **37**, 451 (2020).
10. Y. Zaouter, F. Morin, C. Hoenninger, and E. Mottay, Proc. SPIE **7914**, 79141J (2011).
11. Y. Zaouter, F. Guichard, L. Daniault, M. Hanna, F. Morin, C. Hönninger, E. Mottay, F. Druon, and P. Georges, Opt. Lett. **38**, 106 (2013).
12. C. Stihler, H.-J. Otto, C. Jauregui, J. Limpert, and A. Tünnermann, Proc. SPIE **10083**, 100830R (2017).
13. H.-W. Chen, J. Lim, S.-W. Huang, D. N. Schimpf, F. X. Kärtner, and G. Chang, Opt. Express **20**, 28672 (2012).
14. W. Liu, D. N. Schimpf, T. Eidam, J. Limpert, A. Tunnermann, F. X. Kartner, and G. Chang, Opt. Lett. **40**, 151 (2015).
15. J. Zhao, W. Li, C. Wang, Y. Liu, and H. Zeng, Opt. Express **22**, 32214 (2014).
16. Y. Liu, W. Li, D. Luo, D. Bai, C. Wang, and H. Zeng, Opt. Express **24**, 10939 (2016).
17. H. Song, B. Liu, Y. Li, Y. Song, H. He, L. Chai, M. Hu, and C. Wang, Opt. Express **25**, 7559 (2017).
18. Y. Zhang, R. Chen, H. Huang, Y. Liu, H. Teng, S. Fang, W. Liu, F. Kaertner, J. Wang, G. Chang, and Z. Wei, OSA Contin. **3**, 1988 (2020).
19. S. Zhou, F. W. Wise, and D. G. Ouzounov, Opt. Lett. **32**, 871 (2007).
20. R. Chen and G. Chang, Opt. Express **29**, 6330 (2021).